

# An Obligatory Heterodimer of 14-3-3 $\beta$ and 14-3-3 $\epsilon$ Is Required for Aldosterone Regulation of the Epithelial Sodium Channel\*<sup>§</sup>

Received for publication, May 13, 2008, and in revised form, July 18, 2008. Published, JBC Papers in Press, August 7, 2008, DOI 10.1074/jbc.M803687200

Xiubin Liang, Michael B. Butterworth, Kathryn W. Peters, William H. Walker, and Raymond A. Frizzell<sup>1</sup>

From the Department of Cell Biology and Physiology, University of Pittsburgh School of Medicine, Pittsburgh, Pennsylvania 15261

Increased distal nephron sodium absorption in response to aldosterone involves Nedd4-2 phosphorylation, which blocks its ability to ubiquitylate ENaC and increases apical membrane channel density by reducing its endocytosis. Our prior work (Liang, X., Peters, K. W., Butterworth, M. B., and Frizzell, R. A. (2006) *J. Biol. Chem.* 281, 16323–16332) showed that aldosterone selectively increased 14-3-3 protein isoform expression and that the association of 14-3-3 $\beta$  with phospho-Nedd4-2 was required for sodium transport stimulation. The knockdown of 14-3-3 $\beta$  alone nearly eliminated the response to aldosterone, despite the expression of other 14-3-3 isoforms in cortical collecting duct (CCD) cells. To further examine this marked effect of 14-3-3 $\beta$  knockdown, we evaluated the hypothesis that phospho-Nedd4-2 binding prefers a heterodimer composed of two different 14-3-3 isoforms. We tested this concept in polarized CCD cells using RNA interference and assays of sodium transport and of the interaction of Nedd4-2 with 14-3-3 $\epsilon$ , a second aldosterone-induced isoform. As observed previously for 14-3-3 $\beta$  knockdown, small interfering RNA-induced reduction of 14-3-3 $\epsilon$  markedly attenuated aldosterone-stimulated ENaC expression and sodium transport and increased the interaction of Nedd4-2 with ENaC toward prealdosterone levels. After aldosterone induction, 14-3-3 $\beta$  and 14-3-3 $\epsilon$  were quantitatively co-immunoprecipitated from CCD cell lysates, and the association of both isoforms with Nedd4-2 increased. Finally, the knockdown of either 14-3-3 $\beta$  or 14-3-3 $\epsilon$  reduced the association of Nedd4-2 with the other isoform. We conclude that the two aldosterone-induced 14-3-3 isoforms,  $\beta$  and  $\epsilon$ , interact with phospho-Nedd4-2 as an obligatory heterodimer, blocking its interaction with ENaC and thereby increasing apical ENaC density and sodium transport.

The homeostatic control of salt and water balance occurs primarily through regulation of the rate of sodium absorption

\* This work was supported, in whole or in part, by National Institutes of Health Grants DK54814 and DK72506. This work was also supported by the Cystic Fibrosis Foundation. The costs of publication of this article were defrayed in part by the payment of page charges. This article must therefore be hereby marked "advertisement" in accordance with 18 U.S.C. Section 1734 solely to indicate this fact.

<sup>§</sup> The on-line version of this article (available at <http://www.jbc.org>) contains supplemental Fig. 1.

<sup>1</sup> To whom correspondence should be addressed: Dept. of Cell Biology and Physiology, University of Pittsburgh School of Medicine, S362 BST, 3500 Terrace St., Pittsburgh, PA 15261. Tel.: 412-648-9498; Fax: 412-648-8330; E-mail: frizzell@pitt.edu.

across renal cortical collecting duct (CCD)<sup>2</sup> epithelia, where the epithelial sodium channel, ENaC, provides the limiting entry step in this process (1). ENaC is composed of three homologous subunits,  $\alpha$ ,  $\beta$ , and  $\gamma$  (2, 3), and its significance in fluid balance and blood pressure regulation is demonstrated by ENaC subunit mutations that are found in families with genetic hypertension or salt wasting (4–6).

In response to reduced extracellular fluid volume, aldosterone stimulates distal nephron sodium absorption via coordinated transcriptional regulation of transport and metabolic protein expression (7, 8). One aspect of this response involves the increased expression of ENaC, principally its  $\alpha$ -subunit, whose expression appears to be limiting for the trafficking of functional sodium channels to the apical surface of distal nephron principal cells (9). Once delivered to the apical membrane, the endocytic retrieval and recycling of ENaC are relatively rapid events (10, 11). The internalization of ENaC from the cell surface is dictated largely by protein interactions that involve the recognition of PY motifs at the ENaC subunit C termini by the WW domains of the E3 ubiquitin ligase, Nedd4-2 (neural precursor cell-expressed developmentally down-regulated gene 4 isoform 2). ENaC ubiquitylation facilitates engagement of the channel by the endocytic machinery, which promotes its internalization and can lead subsequently to ENaC degradation (12). Removal of ubiquitin allows the channel to recycle to the apical surface, however (11, 13).

The action of aldosterone to increase sodium absorption across the collecting duct is primarily explained by increases in apical membrane ENaC density and increased apical channel residency that are associated with reduced interactions between ENaC and Nedd4-2. Their reduced interaction is mediated by SGK1 (serum- and glucocorticoid-induced kinase 1), whose expression is augmented as a component of the early response of CCD cells to the steroid. SGK1 phosphorylates sites that correspond to its consensus phosphorylation motif, RXXR(S/T), and there are three such sites within Nedd4-2 (14, 15). This post-translational modification disrupts the ability of Nedd4-2 to bind ENaC and thereby interferes with the channel's ubiquitylation and internalization, resulting in increased cell surface expression and sodium transport.

<sup>2</sup> The abbreviations used are: CCD, cortical collecting duct; ENaC, epithelial sodium channel; SGK1, IP, immunoprecipitation; IB, immunoblot; E3, ubiquitin-protein isopeptide ligase; mCCD, mouse cortical collecting duct; HA, hemagglutinin; siRNA, small interfering RNA; contig, group of overlapping clones.

We (16) and others (17, 18) have demonstrated that 14-3-3 proteins are essential components of ENaC regulation by aldosterone. These proteins associate with SGK1-phosphorylated Nedd4-2 to maintain its phosphorylated/inactive state and thereby obstruct its physical association with ENaC. In prior studies, we detected the expression of five of the seven mammalian 14-3-3 isoforms in mouse cortical collecting duct (mCCD) epithelia by reverse transcription-PCR and immunoblot, and we showed that the expression of the 14-3-3 $\beta$  and  $\epsilon$  isoforms were elevated 3- and 12-fold, respectively, by physiological levels of aldosterone, whereas the expression of other expressed isoforms, 14-3-3 $\gamma$ ,  $\theta$ , and  $\sigma$ , were unaffected by the steroid. We focused on 14-3-3 $\beta$  as the predominant isoform expressed in aldosterone-treated epithelia, and we observed time-dependent increases in 14-3-3 $\beta$  levels during aldosterone stimulation that paralleled the increases in SGK1,  $\alpha$ -ENaC, and phospho-Nedd4-2. Co-immunoprecipitation (co-IP) experiments demonstrated that aldosterone shifted Nedd4-2 from an association with ENaC to an interaction with 14-3-3 $\beta$ . As shown by a site-specific phosphorylation-sensitive antibody, this 14-3-3 isoform interacted with Ser<sup>328</sup> of phosphorylated Nedd4-2 to block ENaC binding.

The physiological significance of the 14-3-3 $\beta$ -phospho-Nedd4-2 interaction was revealed by 14-3-3 $\beta$  knockdown, which increased ENaC-Nedd4-2 interactions to prealdosterone levels, blunted the steroid-induced increase in  $\alpha$ -ENaC expression, and virtually eliminated the aldosterone-induced stimulation of sodium absorption across mCCD epithelia. Thus, the knockdown of 14-3-3 $\beta$  alone markedly suppressed several important features of the aldosterone response, despite the expression of other 14-3-3 isoforms and the parallel induction of 14-3-3 $\epsilon$  expression by the steroid (16).

The binding between a 14-3-3 protein and its substrate is generally triggered by phosphorylation of the target at specific Ser/Thr residues (19). In this manner, the 14-3-3 proteins are key regulators of phosphoprotein targets within a variety of cellular signaling pathways. Structural studies show that 14-3-3 proteins interact with their client proteins as dimers, thus possessing two binding sites for target protein interactions. This arrangement may allow them to bring different regions of the same protein into proximity (20, 21). In addition, it is thought that substrate binding specificity may arise from the formation of an optimal dimer interface between two 14-3-3 monomers (22). Structural studies suggest also that 14-3-3 dimers are especially rigid due to their high helical content, and that their conformation is minimally perturbed during client protein binding. This property permits 14-3-3 proteins to physically deform their binding partners. Thus, the intramolecular binding of a 14-3-3 dimer within Nedd4-2 would be expected to obstruct its ability to interact productively with ENaC, according to the "molecular anvil" hypothesis of 14-3-3 interactions proposed by Yaffe (23).

The rationale for the present study was provided by our finding of the selective induction of two 14-3-3 isoforms,  $\beta$  and  $\epsilon$ , by aldosterone, and the known functional requirement of 14-3-3 proteins for dimer association. We asked whether the marked dependence of aldosterone action on the  $\beta$  isoform, as detected in prior knockdown studies, reflects a binding preference of

phospho-Nedd4-2 for a heterodimer of the two 14-3-3 isoforms whose expression is augmented by steroid treatment.

## EXPERIMENTAL PROCEDURES

**Antibodies**—Antibodies specific for 14-3-3 $\beta$  (A-15), 14-3-3 $\epsilon$  (T-16) were purchased from Santa Cruz Biotechnology (Santa Cruz, CA). Antibodies to Nedd4 were obtained from Upstate Biotechnology, Inc. (Lake Placid, NY). For  $\alpha$ -ENaC, a rabbit polyclonal antibody was raised against an epitope of the extracellular loop as described (16). Secondary antibodies against mouse or rabbit were obtained from Amersham Biosciences. Antibodies to  $\beta$ -actin and the HA epitope were obtained from Sigma.

**Cell Culture**—mpkCCDc14 cells (provided by A. Vandewalle and M. Bens, Institut National de la Santé et de la Recherche Médicale, Paris, France) were grown in flasks (passages 30–40) in defined medium, as described previously (24). The growth medium was composed of equal volumes of Dulbecco's modified Eagle's medium and Ham's F-12, plus 60 nM sodium selenate, 5  $\mu$ g/ml transferrin, 2 mM glutamine, 50 nM dexamethasone, 1 nM triiodothyronine, 10 ng/ml epidermal growth factor, 5  $\mu$ g/ml insulin, 20 mM D-glucose, 2% (v/v) FCS, and 20 mM HEPES, pH 7.4 (reagents from Invitrogen and Sigma). The cells were maintained at 37 °C in 5% CO<sub>2</sub>, 95% air, and the media were changed every second day.

For the transepithelial measurements, mCCD cells were subcultured onto permeable filter supports (0.4- $\mu$ m pore size, 0.33-cm<sup>2</sup> surface area; Transwell; Corning Costar). After  $\sim$ 7 days, a polarized monolayer had developed, as assessed by recordings of open circuit voltage (typically  $\sim$ 50 mV) and transepithelial resistance (typically  $\sim$ 2 kilohms $\cdot$ cm<sup>2</sup>), detected using "chopstick" electrodes (Millipore). For the biochemical experiments, mCCD epithelia were polarized on 4.5-cm<sup>2</sup> filters (Corning) for  $\sim$ 7 days prior to use. To assure a regulatory baseline, the growth medium bathing cells on filters was replaced with a minimal medium of Dulbecco's modified Eagle's medium/F-12 (without drugs or hormones) for at least 24 h prior to experiments. Thereafter, mCCD epithelia were either maintained without additives or treated with aldosterone (10 nM; Sigma). This concentration of aldosterone activates mineralocorticoid receptors in CCD cells (25), and it corresponds to plasma aldosterone levels that can be reached during severe salt restriction (26).

**Co-immunoprecipitation Assays**—Protein assays (BCA; Pierce) ensured that equivalent amounts of protein were used for Western blot analysis and immunoprecipitation. Pre-cleared mCCD cell lysates ( $\sim$ 1 mg of protein) were mixed with the appropriate primary antibodies for 1.5 h at 4 °C in lysis buffer (0.4% deoxycholate acid, 1% Nonidet P-40, 50 mM EDTA, 10 mM Tris-HCl at pH 7.4). Twenty-five  $\mu$ l of washed protein A- or G-Sepharose beads was added to each sample and incubated 1 h at 4 °C with gentle rotation. Immunocomplexes were washed with lysis buffer four times and precipitated by centrifugation at 12,000  $\times$  g for 10 s. The immunocomplexes were resuspended in SDS sample buffer and subjected to immunoblotting (see below). Controls for the immunoprecipitations were performed using a concentration of HA antibody equal to that of the primary precipitating antibody.

## Aldosterone Regulates ENaC via a 14-3-3 Heterodimer

**Immunoblot Analyses**—Equal amounts of protein from either aldosterone-treated or nontreated, polarized mCCD cells or the immunoprecipitates described above were resolved by 10% SDS-PAGE and transferred to polyvinylidene difluoride membranes. Unbound sites were blocked for 1 h at room temperature with 5% (w/v) skim milk powder in TBST (10 mM Tris (pH 8.0), 150 mM NaCl, 0.05% Tween 20). The blots were incubated with primary antibodies (anti-14-3-3 isoforms, each 1:1000; anti-Nedd4-2, 1:1000; anti- $\alpha$ -ENaC, 1:1000; or anti- $\beta$ -actin, 1:3000) at room temperature for 2 h. The blots were then washed three times for 10 min each with TBST and incubated for 1 h with 2  $\mu$ g/ml horseradish peroxidase-conjugated secondary antibodies (1:1000; Amersham Biosciences) in TBST with 5% milk, followed by three TBST washes. The reactive bands were visualized with enhanced chemiluminescence (PerkinElmer Life Sciences) and exposed to x-ray film (Eastman Kodak Co.).  $\beta$ -Actin expression provided an internal control. Immunoblot data were scanned, and band densities were quantified using ImageJ software.

**mCCD Transfection with siRNA**—Control siRNA and siRNA for 14-3-3 $\beta$  and 14-3-3 $\epsilon$  were obtained from Dharmacon Inc. (Chicago, IL) as SMARTpool<sup>®</sup> reagents. The control siRNAs were composed of four nontargeting siRNAs, as provided by the manufacturer. Selective isoform knockdown by this approach was verified (see data). *In vitro* transfections with 14-3-3 or control siRNAs were performed using Lipofectamine 2000 (Invitrogen) according to the manufacturer's instructions. In brief, mCCD cells were seeded onto filters and were transfected with siRNAs when they were ~80% confluent. A total of 100 pmol of siRNA was used for  $5 \times 10^5$  cells in 2 ml of culture medium. The filters were washed 24 h after transfection and then maintained under control conditions or treated with aldosterone (10 nM) for 48 h. Thus, 3 days elapsed between siRNA transfection and the biochemical or functional assays to evaluate the influence of 14-3-3 isoform knockdown on protein expression, protein interactions, or sodium transport. In addition to the siRNA control, the results were compared with data obtained from untreated CCD cells.

**Short Circuit Current Recordings**—Epithelia cultured on filter supports were mounted in modified Using chambers (Costar), and the cultures were continuously short circuited by an automatic voltage clamp (Department of Bioengineering, University of Iowa, Iowa City, IA), as previously described (10). Transepithelial resistance was calculated from Ohm's law using a periodic 2.5-mV bipolar pulse. The bathing solution consisted of 120 mM NaCl, 25 mM NaHCO<sub>3</sub>, 3.3 mM KH<sub>2</sub>PO<sub>4</sub>, 0.8 mM K<sub>2</sub>HPO<sub>4</sub>, 1.2 mM MgCl<sub>2</sub>, 1.2 mM CaCl<sub>2</sub>, and 10 mM D-glucose. Chambers were maintained at 37 °C and gassed continuously with a mixture of 95% O<sub>2</sub>, 5% CO<sub>2</sub>, which fixed the pH at 7.4. Amiloride (10  $\mu$ M) was added to the apical bath to determine ENaC-mediated transepithelial currents.

**Statistical Analysis**—Data were obtained from experiments performed 3–4 times, and values are presented as mean  $\pm$  S.E. *p* values were calculated by analysis of variance, followed by unpaired *t* test as appropriate. A *p* value of <0.05 was considered to be statistically significant.

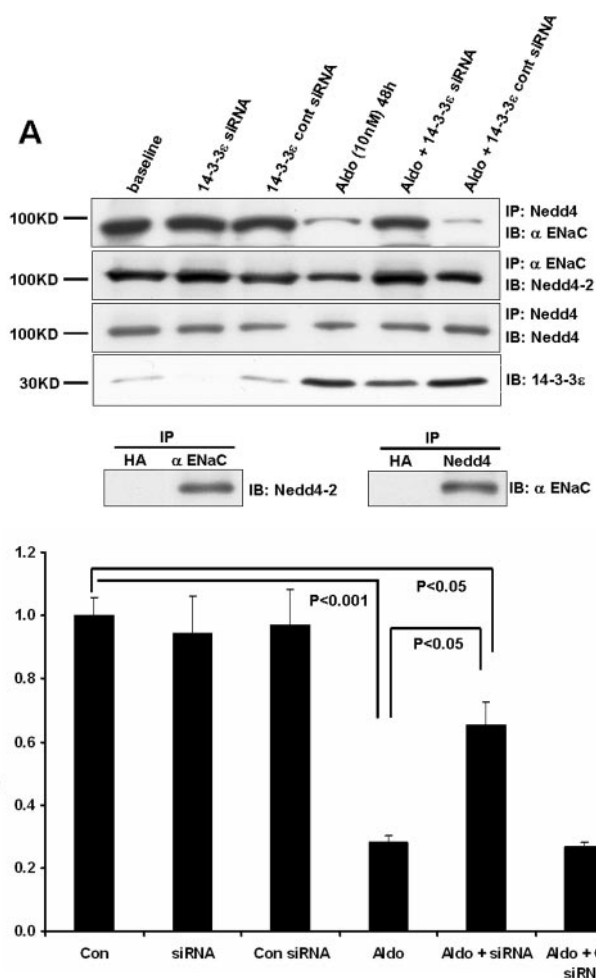


**FIGURE 1. 14-3-3 $\epsilon$  knockdown reverses the aldosterone-induced decrease in Nedd4-2 binding to  $\alpha$ -ENaC.** *A*, pre-confluent mCCD epithelia were transfected with siRNAs targeting 14-3-3 $\epsilon$  expression or with control siRNAs, as described under "Experimental Procedures." Expression of the indicated proteins was determined by immunoblot using mCCD epithelia that had been maintained under control (base-line) conditions or stimulated with 10 nM aldosterone for 48 h before cell lysis. Knockdown of 14-3-3 $\epsilon$  is documented by blots in the *last row*. Co-immunoprecipitations were performed using antibodies against  $\alpha$ -ENaC or Nedd4; binding of Nedd4-2 or  $\alpha$ -ENaC, respectively, was then determined by immunoblot, as shown. Nedd4 IP/IB (*third row*) was performed as a control and for data normalization. IP with an anti-HA IgG was performed as a control and yielded no signal for either Nedd4-2 or  $\alpha$ -ENaC. *B*, densitometric quantitation of results from the Nedd4/ $\alpha$ -ENaC co-IP (row 1) were normalized to bands from the Nedd4 IP/IB, with the control (base-line) level set to unity. Total Nedd4 expression is not influenced by aldosterone (16), making this normalization method possible. Summary data are from three independent experiments.

## RESULTS

**14-3-3 $\epsilon$  Knockdown Increases the Association of ENaC with Nedd4-2**—A significant early manifestation of aldosterone's action is a decrease in the interaction of Nedd4-2 with ENaC, which is associated with the early induction of SGK1 expression and its phosphorylation of Nedd4-2. We previously showed that the interaction of 14-3-3 $\beta$  with SGK1-phosphorylated Nedd4-2 stabilizes the inactive form of the ubiquitin ligase and reduces its interaction with the channel. To evaluate the ability of the other aldosterone-induced isoform, 14-3-3 $\epsilon$ , to interfere with ENaC-Nedd4-2 interactions, we examined the effect of 14-3-3 $\epsilon$  knockdown on the co-IP of  $\alpha$ -ENaC and Nedd4-2 under basal and stimulated conditions (Fig. 1*A*). siRNA-in-

duced reduction in 14-3-3 $\epsilon$  expression in different experiments ranged between 90 and 60% under basal *versus* stimulated conditions (*i.e.* knockdown was less efficient following aldosterone-induced expression of the protein). In this and subsequent experiments, the control siRNA pool had no effect.

The antibodies to Nedd4 used in these co-IP experiments recognize its second WW domain and therefore both the Nedd4-1 and Nedd4-2 isoforms. The complete gel from a Nedd4 blot is provided in supplemental Fig. 1, and it indicates that other WW domain proteins were not detected in mCCD lysates. The small difference in molecular weight of the 4-1 and 4-2 isoforms is not resolved under these conditions, but mCCD cells express both isoforms, and only the latter interacts physically and functionally with ENaC (27). The reported Nedd4 blots and IPs provide data on both isoforms and are labeled *Nedd4*. However, immunoprecipitation of ENaC followed by Nedd4 immunoblot provides data on the selective interaction of ENaC with Nedd4-2 (27), and the blots of these IPs are labeled as such (Fig. 1A).

As observed previously for 14-3-3 $\beta$ , reducing 14-3-3 $\epsilon$  expression did not alter the ENaC-Nedd4-2 interaction at baseline, in the absence of aldosterone treatment. This outcome is probably due to the low levels of phospho-Nedd4-2 that are found in the absence of steroid treatment (16, 28). As anticipated, aldosterone decreased the interaction of Nedd4-2 with  $\alpha$ -ENaC (*lane 1 versus lane 4*), and as with 14-3-3 $\beta$ , the knockdown of 14-3-3 $\epsilon$  reversed this interaction toward levels observed in the absence of steroid. As controls, IP with an anti-HA IgG yielded no signal for either Nedd4-2 or  $\alpha$ -ENaC. Quantitation of the results from all experiments (Fig. 1B) indicated that aldosterone produced a 70% reduction in the amount of Nedd4-2 associated with  $\alpha$ -ENaC, whereas the aldosterone-induced reduction in ENaC-Nedd4-2 binding was reduced to 30% when the expression of 14-3-3 $\epsilon$  was reduced by 60%. Our prior study (16) showed that aldosterone elicited a ~10-fold increase in 14-3-3 $\epsilon$  binding to Nedd4-2. Thus, the present data are consistent with the concept that the association of 14-3-3 $\epsilon$  with phospho-Nedd4-2 blocks the ENaC-Nedd4-2 interaction.

**14-3-3 $\epsilon$  Knockdown Blocks Aldosterone-induced Increases in Sodium Transport**—To evaluate the functional impact of reduced 14-3-3 $\epsilon$  on ENaC-mediated sodium absorption, we determined the amiloride-sensitive currents across mCCD epithelia under basal conditions and after transfection with 14-3-3 $\epsilon$  or control siRNAs. During the next 48 h, mCCD epithelia remained under basal conditions or were treated with aldosterone. Fig. 2 shows typical transepithelial current records (Fig. 2A) and summary data of the amiloride-sensitive short circuit current ( $I_{sc}$ ), which was increased by aldosterone 2.2-fold (Fig. 2B). The control siRNA treatment had no significant effect on either basal current or the current response to aldosterone. In the absence of aldosterone, 14-3-3 $\epsilon$  siRNA had no effect on  $I_{sc}$ , as observed for ENaC-Nedd4-2 interactions (see above). Also, similar to the data of Fig. 1, and as found previously for 14-3-3 $\beta$  knockdown (16), treatment with siRNA targeting 14-3-3 $\epsilon$  expression essentially abolished aldosterone-stimulated sodium absorption. In other words, the  $I_{sc}$  values from basal and aldosterone-treated epithelia after 14-3-3 $\epsilon$  knockdown were not statistically different. The basis of the dis-

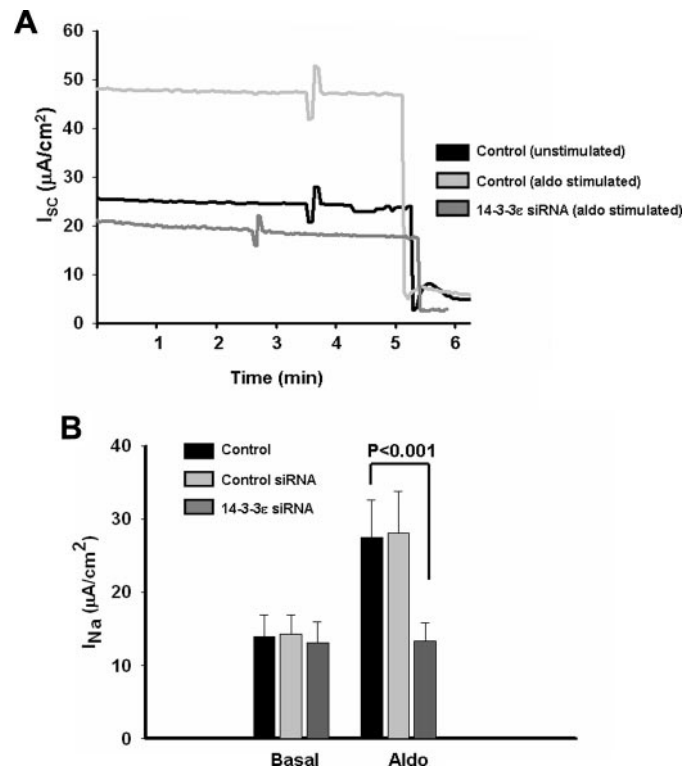


**FIGURE 2. 14-3-3 $\epsilon$  knockdown blocks aldosterone-induced sodium transport across mCCD epithelia.** Experimental conditions for 14-3-3 $\epsilon$  knockdown were as in Fig. 1. *A*, typical traces of short circuit current ( $I_{sc}$ ;  $\mu A/cm^2$ ) across mCCD epithelia under control conditions or 48 h after treatment with aldosterone (10 nM), using control or 14-3-3 $\epsilon$  siRNA-transfected epithelia, as indicated. The abrupt drop in  $I_{sc}$  is elicited by the apical addition of amiloride (10  $\mu M$ ). *B*, amiloride-sensitive  $I_{Na}$  from all experiments of the type shown in *A*. Summary data are from eight epithelia studied under each condition.

proportionate effect on sodium absorption of a ~60% knockdown of 14-3-3 isoforms is not known; however, preliminary data suggest that other steps in the aldosterone-stimulated ENaC trafficking pathway involve mediation by 14-3-3 proteins.<sup>3</sup> Thus, the cumulative effect of inhibition at serial steps in the trafficking pathway could yield a large net effect on apical ENaC density relative to that expected from inhibition at a single site. Nevertheless, together with the biochemical data of Fig. 1, these findings highlight the physiological requirement for 14-3-3 $\epsilon$  in the sodium transport response to aldosterone.

**14-3-3 $\epsilon$  Knockdown Reverses the Aldosterone-induced Increase in ENaC Expression**—A significant action of aldosterone to elevate ENaC-mediated sodium transport involves increased channel expression. At least in part, this effect is due to increased transcriptional production of channel subunits by the steroid (9, 29, 30). As shown in Fig. 3, aldosterone treatment of mCCD epithelia produced a 5–6-fold increase in expression of  $\alpha$ -ENaC. As previously reported (16), aldosterone also increased the steady-state expression of 14-3-3 $\beta$  and 14-3-3 $\epsilon$ . The expression of 14-3-3 $\epsilon$  under basal conditions was weakly detectable, and aldosterone increased its expression ~10-fold. The significance of 14-3-3 $\epsilon$  in the response of  $\alpha$ -ENaC expression was evaluated using 14-3-3 $\epsilon$ -targeted siRNAs in polarized

<sup>3</sup> X. Liang, M. B. Butterworth, K. W. Peters, W. H. Walker, and R. A. Frizzell, unpublished data.

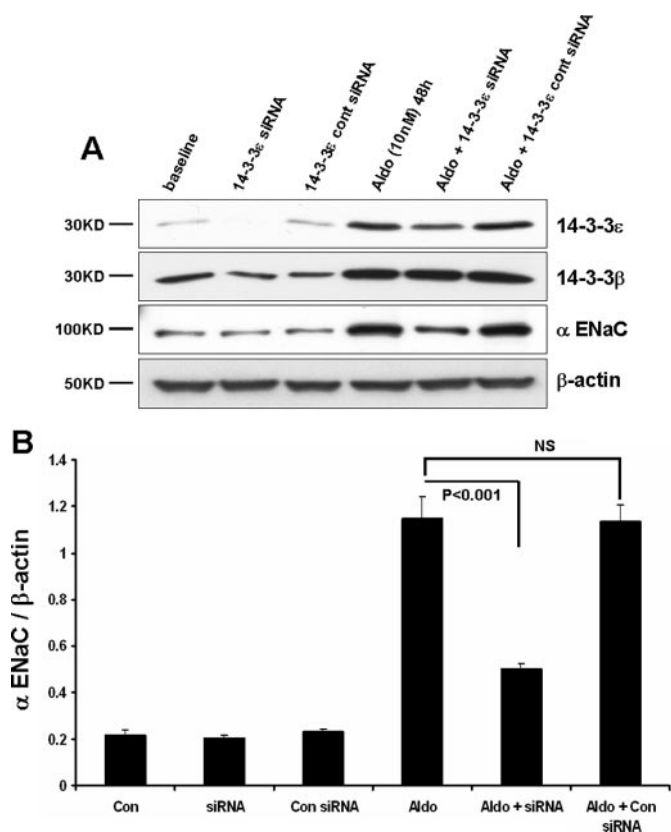


**FIGURE 3. 14-3-3 $\epsilon$  knockdown reduces aldosterone-stimulated  $\alpha$ -ENaC expression.** Experimental conditions for 14-3-3 $\epsilon$  knockdown were as in Fig. 1. *A*, expression of the indicated proteins was determined by immunoblot using mCCD epithelia that had been maintained under control (base-line) conditions or stimulated with 10 nM aldosterone for 48 h before cell lysis. *B*, quantitation of  $\alpha$ -ENaC expression as a function of experimental condition from three experiments of the type shown in *A*.

mCCD cells. Importantly, 14-3-3 $\epsilon$  knockdown was selective and did not affect the expression of 14-3-3 $\beta$  (Fig. 3*A*).

The influence of 14-3-3 $\epsilon$  knockdown on the expression of  $\alpha$ -ENaC is illustrated by the blots of Fig. 3*A* and the quantitation of the complete data set, provided in Fig. 3*B*. In nonstimulated cells, a reduction in 14-3-3 $\epsilon$  did not alter  $\alpha$ -ENaC expression, again indicating that this 14-3-3 isoform does not play a significant role under nonstimulated conditions. In stimulated cells, the increase in  $\alpha$ -ENaC expression observed with aldosterone treatment was blunted 65% in cells with reduced 14-3-3 $\epsilon$ . The ~2-fold elevation of  $\alpha$ -ENaC remaining after 14-3-3 $\epsilon$  knockdown probably reflects the influence of aldosterone on the transcription of this ENaC subunit.

Together, the data of Figs. 1–3 indicate that 14-3-3 $\epsilon$  participates in the regulation of apical membrane ENaC density by aldosterone, similar to findings previously published for 14-3-3 $\beta$ , the other aldosterone-induced isoform in mCCD epithelia. In view of the disproportionate biochemical and functional effects of 14-3-3 knockdown, and since these proteins act as dimers (31), we asked whether 14-3-3 $\beta$  and 14-3-3 $\epsilon$  associate with one another in mCCD cells and act as a heterodimer in their interaction with phospho-Nedd4-2.

**14-3-3 $\beta$  and 14-3-3 $\epsilon$  Interact *in Vivo***—To determine the extent of endogenous 14-3-3 $\beta$  and 14-3-3 $\epsilon$  interactions, we performed co-immunoprecipitation experiments using cell

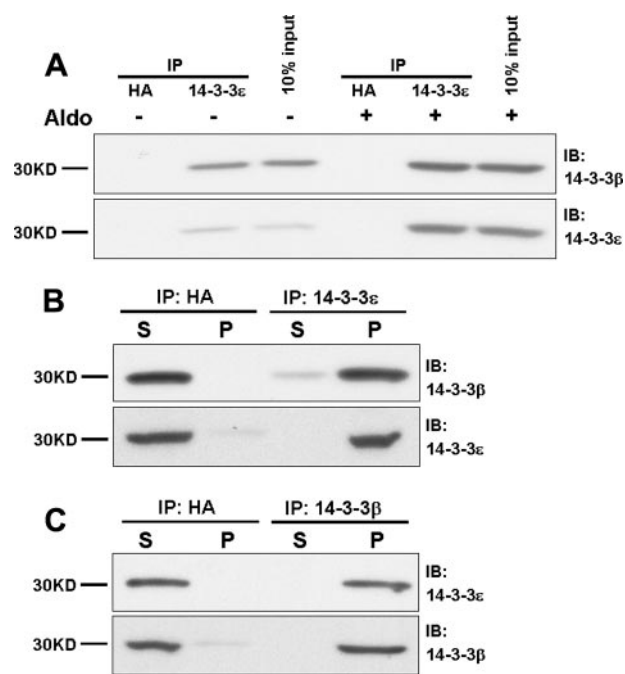


**FIGURE 4. 14-3-3 $\beta$  and 14-3-3 $\epsilon$  interact directly *in vivo*.** Interactions of 14-3-3 $\epsilon$  with 14-3-3 $\beta$  were evaluated using lysates from mCCD epithelia obtained under basal conditions and after treatment with aldosterone (10 nM) for 48 h. *A*, the IPs employed antibodies to 14-3-3 $\epsilon$  or, as control, to the HA epitope; binding of 14-3-3 $\beta$  was determined by immunoblot. *B*, immunoblots for 14-3-3 $\beta$  or  $\epsilon$  were performed using the supernatant (S) or solubilized pellet (P) derived from IP experiments for 14-3-3 $\epsilon$  in CCD epithelia treated with aldosterone for 48 h. *C*, IP similar to *B* was performed using antibodies against 14-3-3 $\beta$  followed by blot of 14-3-3 $\epsilon$  in supernatant or pellet. The data are representative of results from three experiments.

lysates from polarized mCCD epithelia. Protein complexes were isolated from epithelia maintained under basal or aldosterone-treated conditions using anti-14-3-3 $\epsilon$ , resolved by SDS-PAGE, and blotted for 14-3-3 $\beta$ . Representative data are illustrated in Fig. 4*A*. IPs performed with an anti-HA IgG as control yielded no 14-3-3 $\beta$  or  $\epsilon$  signal in the presence or absence of steroid. Under basal nonstimulated conditions, a modest amount of 14-3-3 $\beta$  was precipitated with 14-3-3 $\epsilon$ . As shown by the input (see also Figs. 1 and 3), the expression of 14-3-3 $\epsilon$  is relatively low in the absence of aldosterone. Relative to basal conditions, aldosterone increased the expression of both 14-3-3 $\epsilon$  and 14-3-3 $\beta$  and increased the association of these isoforms with one another.

Further evidence of a strict interaction between 14-3-3 $\beta$  and 14-3-3 $\epsilon$  following aldosterone treatment was provided by comparisons of the 14-3-3 $\beta$  content of supernatant and pellet following IP of 14-3-3 $\epsilon$ , as illustrated in Fig. 4*B*. The blots show that the IP-induced depletion of 14-3-3 $\epsilon$  from the supernatant is paralleled by the nearly complete depletion of 14-3-3 $\beta$ , providing evidence of a stoichiometric interaction between these isoforms in aldosterone-treated epithelia. As shown in Fig. 4*C*, a similar quantitative depletion of 14-3-3 $\epsilon$  from the supernatant occurred when 14-3-3 $\beta$  was removed by IP. These findings provide strong evidence for the *in vivo* assembly of a heterodimer of 14-3-3 $\beta$  and 14-3-3 $\epsilon$ , the two isoforms whose expression is induced by aldosterone.

**14-3-3 Isoforms Interact with Nedd4-2 *in Vivo***—In separate co-immunoprecipitation experiments, we showed previously

that 14-3-3 $\beta$  or 14-3-3 $\epsilon$  interact with Nedd4-2 *in vivo* (16). The effect of aldosterone on these interactions is illustrated in Fig. 5. Co-IP experiments were performed using lysates from polarized mCCD epithelia under basal and aldosterone-treated conditions. Protein complexes were isolated using anti-Nedd4, resolved by SDS-PAGE, and blotted with antibodies to 14-3-3 $\beta$  or - $\epsilon$ . IPs performed with an anti-HA IgG as control yielded no 14-3-3 signal. In our prior study (16), preincubation of cell lysates with an antibody directed at Nedd4-2 phosphoserine 328 blocked its interaction with 14-3-3 $\beta$ , indicating that 14-3-3 binding requires an interaction at this phosphorylated residue. Since this site is absent in Nedd4-1 (27), co-IPs performed with

the Nedd4 antibody will detect only the interaction of 14-3-3s with Nedd4-2.

Under basal conditions, associations of 14-3-3 $\beta$  or 14-3-3 $\epsilon$  with Nedd4-2 were not detected; however, their interactions were readily observed following aldosterone treatment. The negligible interaction of Nedd4-2 with these 14-3-3 isoforms under basal conditions explains the absence of effects of 14-3-3 knockdown in the absence of steroid treatment (Figs. 1–3). The findings of Fig. 5 set the stage for examining the interdependence of isoform interactions with Nedd4-2 using selective isoform knockdown.

*Isoform Knockdown Affects Nedd4-2 Binding of the Other Isoform*—Since the knockdown of either 14-3-3 $\beta$  or 14-3-3 $\epsilon$  markedly reduced aldosterone-simulated increases in ENaC expression and current, we asked whether a reduction in the expression of one isoform would abrogate binding of the other isoform by Nedd4-2. As shown in Fig. 6, *A* and *B*, the siRNA-mediated knockdown of 14-3-3 $\beta$  expression led to a reduction not only of the extent of 14-3-3 $\beta$  binding by Nedd4-2 but also to a decrease in its interaction with 14-3-3 $\epsilon$ . This reduction in 14-3-3 $\epsilon$  binding was restricted to aldosterone-treated epithelia, as observed previously for the functional effects of isoform knockdown, and its magnitude ( $\sim 60\%$ ) was quantitatively similar to the reduction in 14-3-3 $\beta$  binding by Nedd4-2.

Similarly, as shown in Fig. 6, *C* and *D*, the knockdown of 14-3-3 $\epsilon$  expression led to reductions in the association of both

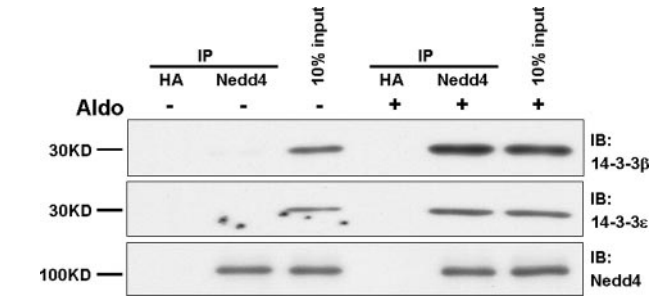


FIGURE 5. 14-3-3 $\beta$  and  $\epsilon$  interact with Nedd4-2 *in vivo*. Interactions of 14-3-3 $\beta$  and  $\epsilon$  with Nedd4-2 were evaluated using lysates from mCCD epithelia obtained under basal conditions and after treatment with aldosterone (10 nM) for 48 h. The IPs employed antibodies to Nedd4-2 or, as control, the HA epitope, followed by 14-3-3 isoform blot. Data are representative of the results from three experiments.

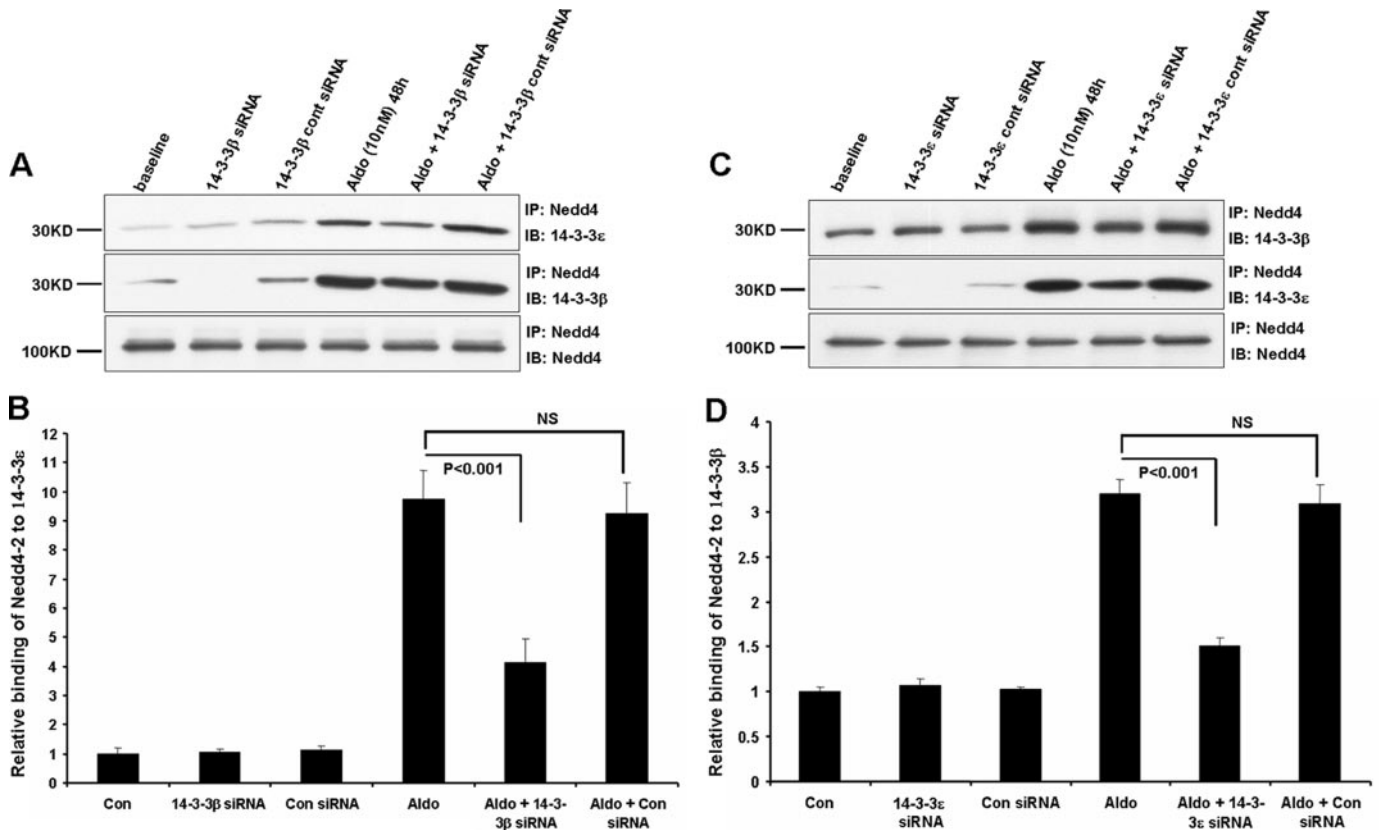


FIGURE 6. Effect of 14-3-3 $\beta$  or  $\epsilon$  knockdown on their interaction with Nedd4-2. Experimental conditions were as in Fig. 1. *A*, knockdown of 14-3-3 $\beta$ ; immunoprecipitations were performed using antibodies against Nedd4 and binding of 14-3-3 $\beta$  or - $\epsilon$  determined by immunoblot, as shown. Nedd4-2 IP/IB (*last row*) was performed as a control. *B*, quantitation of summary data from three independent experiments; normalization was performed as for Fig. 1B. *C*, knockdown of 14-3-3 $\epsilon$ ; immunoprecipitations were performed using antibodies against Nedd4, and binding of 14-3-3 $\beta$  or - $\epsilon$  was determined by immunoblot. Nedd4 IP/IB (*last row*) was performed as a control and for data normalization. *D*, quantitation of data (as above) from three independent experiments.

## Aldosterone Regulates ENaC via a 14-3-3 Heterodimer

14-3-3 $\epsilon$  and 14-3-3 $\beta$  with Nedd4-2, and these effects were observed only after aldosterone treatment. As observed above, the ~80% reduction in 14-3-3 $\epsilon$  binding to Nedd4-2 with 14-3-3 $\beta$  knockdown was similar to the decrease in 14-3-3 $\beta$  binding. These findings indicate that 14-3-3 $\beta$  and 14-3-3 $\epsilon$  act as a heterodimer in their interaction with phosphorylated Nedd4-2 to support the action of aldosterone in augmenting ENaC-mediated sodium absorption.

### DISCUSSION

ENaC is of fundamental importance in the control of sodium absorption in a variety of epithelial tissues, including the kidney, lung, exocrine gland ducts, and colon (32). Thus, ENaC activity is an important determinant in the control of sodium balance, blood pressure, and airway surface liquid clearance (33). As such, ENaC is a principal target in the hormonal regulation of sodium retention by aldosterone, vasopressin, and insulin (34). The aldosterone-induced expression of the serine-threonine kinase SGK1 represents a central control point in the molecular mechanism of the steroid's actions. The rapid induction of SGK1 (<1 h) leads to phosphorylation of the E3 ubiquitin ligase, Nedd4-2, which reduces its affinity for ENaC binding and thereby reduces ubiquitin-mediated channel endocytosis and degradation (14, 35).

Important in the maintenance of this response is the interaction of phosphorylated Nedd4-2 with 14-3-3 proteins (16, 18). We previously determined the expression of 14-3-3 isoforms in aldosterone-responsive, mpkCCDC14 epithelia and showed that the expression of two isoforms, 14-3-3 $\beta$  and  $\epsilon$ , was induced by treatment with physiological aldosterone concentrations. The induction of 14-3-3 $\beta$  expression by aldosterone paralleled that of SGK1,  $\alpha$ -ENaC, and phosphorylated Nedd4-2 over the 48-h time course examined (16).

Although the upstream regulatory sequences for 14-3-3 proteins are poorly explored, we have examined the 1,000-bp region directly upstream of the transcription start site for 14-3-3 $\beta$  on contig AL591542.20.1.197190 from the Ensembl mouse genome sequence data base. Analysis of this putative promoter region using Transcription Element Search System software identified several glucocorticoid receptor consensus binding sites. Due to overlapping consensus sequences, some of the glucocorticoid receptor binding motifs contain half-site consensus binding motifs for mineralocorticoid receptors. It has become evident that the regulation of transcription by steroid hormone receptors, including the mineralocorticoid receptors, is complex and regulated by interacting signaling networks (36). Whether these upstream loci account for the aldosterone-induced expression of 14-3-3 $\beta$  will require more extensive analysis.

RNAi-mediated silencing of 14-3-3 $\beta$  expression blunted the aldosterone-induced increases in  $\alpha$ -ENaC expression, its association with Nedd4-2, and sodium absorption rate (16). The large magnitude of the responses to 14-3-3 $\beta$  knockdown prompted the present study to determine whether a heterodimer of the two aldosterone-induced isoforms,  $\beta$  and  $\epsilon$ , might be responsible for the stabilization of phospho-Nedd4-2. Consistent with this concept, we found that the knockdown of 14-3-3 $\epsilon$  expression also abrogated several actions of aldoster-

one, including its ability to suppress the interaction between ENaC and Nedd4-2 (Fig. 1), its stimulation of sodium transport (Fig. 2), and ENaC subunit expression (Fig. 3). Although aldosterone is known to augment ENaC transcription (9), the large decreases in ENaC expression that resulted from the knockdown of 14-3-3 $\beta$  or  $\epsilon$  (Fig. 3) (16) highlight the significance of ENaC stabilization at the apical membrane by the inhibitory action of the 14-3-3 proteins on Nedd4-2.

The absence of these effects of 14-3-3 isoform knockdown under basal conditions appears to be due to the low level of SGK1 expression and the correspondingly low levels of Nedd4-2 phosphorylation, as found previously (16). A minor amount of 14-3-3 $\beta$  and  $\epsilon$  interaction was detected under basal conditions (Fig. 4), but in the absence of aldosterone, no significant association of either isoform with Nedd4-2 was observed (Fig. 5). Rather, these interactions were encouraged by aldosterone, due to its stimulation of SGK1, 14-3-3 $\beta$ , and 14-3-3 $\epsilon$  expression. Therefore, our findings indicate that, as for 14-3-3 $\beta$ , 14-3-3 $\epsilon$  participates in the regulation of apical ENaC density by aldosterone, providing direct evidence that a heterodimer of these isoforms interacts with phospho-Nedd4-2. The heterodimer stabilizes the phosphorylated state of Nedd4-2, physically blocks its association with ENaC, and thereby reduces ubiquitination and endocytic retrieval of the channel.

**14-3-3 Dimer Formation**—In the presence of aldosterone, the *in vivo* interactions of 14-3-3 $\beta$  and  $\epsilon$  were direct and stoichiometric (Fig. 4). The immunoprecipitation of either isoform quantitatively depleted the other isoform from mCCD supernatants. Also, reducing 14-3-3 $\beta$  expression decreased the interaction of Nedd4-2 with 14-3-3 $\epsilon$ , and reducing 14-3-3 $\epsilon$  expression decreased the interaction of Nedd4-2 with 14-3-3 $\beta$ .

The 14-3-3s were the first family of proteins to be regarded as phosphoserine/threonine binding modules. Initial studies to determine 14-3-3 binding sites revealed that their optimal target sequences could be characterized as either mode-1 (RSX-pSXP; where pS represents phosphoserine) or mode-2 (RXXX-pSXP) (19, 37). Using a genetic screen, Coblitz *et al.* (38) identified the C-terminal sequence SWpTX as a "mode-3" 14-3-3 binding motif (38). This collection of target sites is described as canonical, but variations on these motifs have also been documented to mediate 14-3-3 protein interactions with substrates (39). The human genome contains seven distinct 14-3-3 genes denoted  $\beta$ ,  $\gamma$ ,  $\epsilon$ ,  $\eta$ ,  $\sigma$ ,  $\theta$ , and  $\zeta$ , and structural studies have shown that these proteins interact with their phospho-binding sites exclusively as dimers (31). Some isoforms prefer to adopt strictly homodimeric interactions, such as human 14-3-3 $\sigma$  and  $\gamma$  (40, 41), whereas others have been implicated in preferential heterodimer formation, such as human 14-3-3 $\epsilon$  (42). Dimeric 14-3-3s bind to a wide variety of proteins to regulate and coordinate a diverse array of cellular processes, such as protein trafficking, signal transduction, cytoskeletal rearrangements, etc. It has remained largely unresolved how 14-3-3 proteins exhibit specificity toward the binding and regulation of a diverse set of targets that are involved in many different signaling pathways; however, structural studies have provided important clues to this process.

The human 14-3-3 $\theta$  (43) and 14-3-3 $\zeta$  (44) crystal structures, first reported in 1995, revealed that 14-3-3 proteins form a

dimer resembling a flattened horseshoe with a central cavity,  $35 \times 35 \text{ \AA}$  and  $20 \text{ \AA}$  deep, that contains two phosphoprotein binding sites. Each monomeric subunit is composed of nine antiparallel  $\alpha$ -helices (identified as  $\alpha A$ – $\alpha I$ ). Residues within the first four  $\alpha$ -helices form the dimer interface ( $\alpha A$ ,  $\alpha B$ ,  $\alpha C$ , and  $\alpha D$ ), as well as the floor of the cavity. Helices  $\alpha A$  and  $\alpha B$  from one monomer interact with  $\alpha C'$  and  $\alpha D'$  of the other monomer across the dimer interface. Three salt bridges involving Arg<sup>18</sup>–Glu<sup>89</sup>, Glu<sup>5</sup>–Lys<sup>74</sup>, and Asp<sup>21</sup>–Lys<sup>85</sup>, as well as several buried polar and hydrophobic residues, are involved in maintaining the homodimer interface in the  $\zeta$  isoform (44). The first salt bridge and all of the key hydrophobic/polar contacts are conserved in all human 14-3-3 isotypes. However, the second salt bridge is absent in  $\sigma$ ,  $\eta$ ,  $\epsilon$ , and  $\gamma$  isoforms, and the third salt bridge is present in all human 14-3-3 structures except  $\epsilon$ . Thus, the potential for formation of only one, rather than three, salt bridges across the interface of a 14-3-3 $\epsilon$  homodimer probably accounts for its propensity to form heterodimers with other isoforms. This property is predicted to discourage  $\epsilon$  homodimer formation but would allow up to two additional salt bridges to form at the interface of a heterodimer of 14-3-3 $\epsilon$  with other isoforms (31).

These considerations are entirely consistent with the implications, from the present study, that aldosterone induces the selective expression of two 14-3-3 isoforms that strongly associate with one another *in vivo* and that this heterodimer has a binding preference for phospho-Nedd4-2. In prior work (16), we demonstrated that incubation of cell lysates with an antibody directed at phosphoserine 328 of mouse Nedd4-2 eliminated the interaction of 14-3-3 $\beta$  with Nedd4-2 in co-IP experiments. In total, there are three SGK1 phosphorylation sites in mNedd4-2 that represent candidate sites for an intramolecular interaction with the 14-3-3 $\beta/\epsilon$  heterodimer. Indeed, 14-3-3s primarily exhibit intramolecular interactions with their targets (39), making it likely that the  $\beta/\epsilon$  heterodimer associates with phospho-Ser<sup>328</sup> as well as another phosphorylation site within Nedd4-2 to distort its conformation and thereby its ability to interact with ENaC.

*Acknowledgments*—We thank Dr. Fei Sun for advice on technical issues and Chloe King for assistance.

## REFERENCES

- Butterworth, M. B., Edinger, R. S., Frizzell, R. A., and Johnson, J. P. (2008) *Am. J. Physiol.*, in press
- Canessa, C. M., Horisberger, J. D., and Rossier, B. C. (1993) *Nature* **361**, 467–470
- Canessa, C. M., Schild, L., Buell, G., Thorens, B., Gautschi, I., Horisberger, J. D., and Rossier, B. C. (1994) *Nature* **367**, 463–467
- Bonny, O., and Rossier, B. C. (2002) *J. Am. Soc. Nephrol.* **13**, 2399–2414
- Lifton, R. P., Gharavi, A. G., and Geller, D. S. (2001) *Cell* **104**, 545–556
- Lifton, R. P. (2004) *Harvey Lect* **100**, 71–101
- Stokes, J. B. (1999) *Kidney Int.* **56**, 2318–2333
- Stockand, J. D. (2002) *Am. J. Physiol.* **282**, F559–F576
- Loffing, J., Zecevic, M., Feraille, E., Kaissling, B., Asher, C., Rossier, B. C., Firestone, G. L., Pearce, D., and Verrey, F. (2001) *Am. J. Physiol.* **280**, F675–F682
- Butterworth, M. B., Edinger, R. S., Johnson, J. P., and Frizzell, R. A. (2005) *J. Gen. Physiol.* **125**, 81–101
- Butterworth, M. B., Edinger, R. S., Ovaa, H., Burg, D., Johnson, J. P., and Frizzell, R. A. (2007) *J. Biol. Chem.* **282**, 37885–37893
- Zhou, R., Patel, S. V., and Snyder, P. M. (2007) *J. Biol. Chem.* **282**, 20207–20212
- Fakitsas, P., Adam, G., Daidie, D., van Bemmelen, M. X., Fouladkou, F., Patrignani, A., Wagner, U., Warth, R., Camargo, S. M., Staub, O., and Verrey, F. (2007) *J. Am. Soc. Nephrol.* **18**, 1084–1092
- Debonneville, C., Flores, S. Y., Kamynina, E., Plant, P. J., Tauxe, C., Thomas, M. A., Munster, C., Chraïbi, A., Pratt, J. H., Horisberger, J.-D., Pearce, D., Loffing, J., and Staub, O. (2001) *EMBO J.* **20**, 7052–7059
- Staub, O., Dho, S., Henry, P., Correa, J., Ishikawa, T., McGlade, J., and Rotin, D. (1996) *EMBO J.* **15**, 2371–2380
- Liang, X., Peters, K. W., Butterworth, M. B., and Frizzell, R. A. (2006) *J. Biol. Chem.* **281**, 16323–16332
- Ichimura, T., Yamamura, H., Sasamoto, K., Tominaga, Y., Taoka, M., Kakiuchi, K., Shinkawa, T., Takahashi, N., Shimada, S., and Isobe, T. (2005) *J. Biol. Chem.* **280**, 13187–13194
- Bhalla, V., Daidie, D., Li, H., Pao, A. C., LaGrange, L. P., Wang, J., Vandewalle, A., Stockand, J. D., Staub, O., and Pearce, D. (2005) *Mol. Endocrinol.* **19**, 3073–3084
- Muslin, A. J., Tanner, J. W., Allen, P. M., and Shaw, A. S. (1996) *Cell* **84**, 889–897
- Wilker, E., and Yaffe, M. B. (2004) *J. Mol. Cell Cardiol.* **37**, 633–642
- Aitken, A., Baxter, H., Dubois, T., Clokie, S., Mackie, S., Mitchell, K., Peden, A., and Zemlickova, E. (2002) *Biochem. Soc. Trans.* **30**, 351–360
- Rimessi, A., Coletto, L., Pinton, P., Rizzuto, R., Brini, M., and Carafoli, E. (2005) *J. Biol. Chem.* **280**, 37195–37203
- Yaffe, M. B. (2002) *FEBS Lett.* **513**, 53–57
- Vinciguerra, M., Deschenes, G., Hasler, U., Mordasini, D., Rousselot, M., Doucet, A., Vandewalle, A., Martin, P. Y., and Feraille, E. (2003) *Mol. Biol. Cell* **14**, 2677–2688
- Naray-Fejes-Toth, A., Helms, M. N., Stokes, J. B., and Fejes-Toth, G. (2004) *Mol. Cell. Endocrinol.* **217**, 197–202
- Hou, J., Speirs, H. J., Seckl, J. R., and Brown, R. W. (2002) *J. Am. Soc. Nephrol.* **13**, 1190–1198
- Kamynina, E., Debonneville, C., Bens, M., Vandewalle, A., and Staub, O. (2001) *FASEB J.* **15**, 204–214
- Staub, O., and Verrey, F. (2005) *J. Am. Soc. Nephrol.* **16**, 3167–3174
- Ergonul, Z., Frindt, G., and Palmer, L. G. (2006) *Am. J. Physiol.* **291**, F683–F693
- Masilamani, S., Kim, G. H., Mitchell, C., Wade, J. B., and Knepper, M. A. (1999) *J. Clin. Invest.* **104**, R19–R23
- Gardino, A. K., Smerdon, S. J., and Yaffe, M. B. (2006) *Semin. Cancer Biol.* **16**, 173–182
- Garty, H., and Palmer, L. G. (1997) *Physiol. Rev.* **77**, 359–396
- Sagnella, G. A., and Swift, P. A. (2006) *Curr. Pharm. Des.* **12**, 2221–2234
- Wang, J., Barbry, P., Maiyar, A. C., Rozansky, D. J., Bhargava, A., Leong, M., Firestone, G. L., and Pearce, D. (2001) *Am. J. Physiol.* **280**, F303–F313
- Snyder, P. M., Steines, J. C., and Olson, D. R. (2004) *J. Biol. Chem.* **279**, 5042–5046
- Pfau, A., Grossmann, C., Freudinger, R., Mildnerberger, S., Benesic, A., and Gekle, M. (2007) *Mol. Cell. Endocrinol.* **264**, 35–43
- Yaffe, M. B., Rittinger, K., Volinia, S., Caron, P. R., Aitken, A., Leffers, H., Gamblin, S. J., Smerdon, S. J., and Cantley, L. C. (1997) *Cell* **91**, 961–971
- Coblitz, B., Shikano, S., Wu, M., Gabelli, S. B., Cockrell, L. M., Spieker, M., Hanyu, Y., Fu, H., Amzel, L. M., and Li, M. (2005) *J. Biol. Chem.* **280**, 36263–36272
- Bridges, D., and Moorhead, G. B. (2005) *Sci. STKE* 2005, re10
- Benzinger, A., Popowicz, G. M., Joy, J. K., Majumdar, S., Holak, T. A., and Hermeking, H. (2005) *Cell Res.* **15**, 219–227
- Wilker, E. W., Grant, R. A., Artim, S. C., and Yaffe, M. B. (2005) *J. Biol. Chem.* **280**, 18891–18898
- Chaudhri, M., Scarabel, M., and Aitken, A. (2003) *Biochem. Biophys. Res. Commun.* **300**, 679–685
- Xiao, B., Smerdon, S. J., Jones, D. H., Dodson, G. G., Soneji, Y., Aitken, A., and Gamblin, S. J. (1995) *Nature* **376**, 188–191
- Liu, D., Bienkowska, J., Petosa, C., Collier, R. J., Fu, H., and Liddington, R. (1995) *Nature* **376**, 191–194